OThJ4.pdf

Carrier Recovery and Equalization for Photonic-Wireless Links with Capacities up to 40 Gb/s in 75-110 GHz Band

Darko Zibar[1], Rakesh Sambaraju[2], Antonio Caballero[2], Javier Herrera[1] and Idelfonso Tafur Monroy[1]
1.DTU Fotonik, Technical University of Denmark, Oersteds Plads Building 343, DK-2800 Kgs. Lyngby, Denmark
2.Valencia Nanophotonics Technol. Center, Universidad Politécnica de Valencia, Camino de Vera s/n, Ed.8F,46022Valencia, Spain.
E-mail: dazi@fotonik.dtu.dk

Abstract: Novel robust digital carrier phase/frequency recovery structure is experimentally demonstrated for single carrier and multi-carrier, up to 40Gb/s, photonic-wireless links in 75-110 GHz band. We show that nonlinear equalization also improves system performance
OCIS codes: (060.1660) Coherent communications; (060.5625) Radio frequency photonics

1. Introduction

Currently, there is a lot of research effort to realize high-capacity wireless link with the capacities approaching that of baseband optical links [1-3]. In order to realize very high capacity wireless links, millimeter wave frequency bands (60 GHz, 75 GHz –110 GHz, 120 GHz etc) are very attractive due to several GHz of available bandwidth. One of the major challenges is generation of multilevel wireless signals with capacities beyond 10 Gb/s and their subsequent demodulation, at millimeter wave frequencies using RF electronics, [2-3]. Therefore, there is a great opportunity for photonic techniques to realize high-capacity wireless links beyond 10 Gb/s.

We have very recently proposed a novel technique based on photonic heterodyne mixing and digital coherent detection to generate and demodulate wireless signals up to 40 Gb/s in 75 GHz – 110 GHz band [4]. The main idea is to convert a high capacity optical baseband single carrier or multi-carrier signal to a wireless signal by simple heterodyning in a photodiode and perform RF transparent digital signal processing based coherent detection at the receiver [4]. However, the digital demodulation, in terms of frequency and phase recovery, at the receiver becomes very challenging due to large laser frequency offsets and significantly increased total phase noise. This is because in our proposed scheme[], we have four free-running lasers beating and therefore very robust demodulation algorithms are required. Additionally, signal distortions in terms of bandwidth limitation and components nonlinearities, limit the demodulation even further requiring advanced equalization techniques. In this paper, we propose and experimentally demonstrate a novel digital carrier phase and frequency recovery structure which is a hybrid between Viterbi &Viterbi (V&V) algorithm and digital phase-locked loop for signal demodulation up to 40 Gb/s in 75 GHz – 110 GHz band. A robust behavior is experimentally demonstrated. Additionally, we experimentally demonstrate that by employing a nonlinear equalizer such as a Decision Feedback Equalizer (DFE), the overall system performance can be improved by mitigating some of the components nonlinearities.

2. Experimental set-up

The experimental set-up for generation and demodulation of single carrier and multi-carrier (OFDM) wireless signal in the 75 GHz – 110 GHz band is shown in Fig .1.

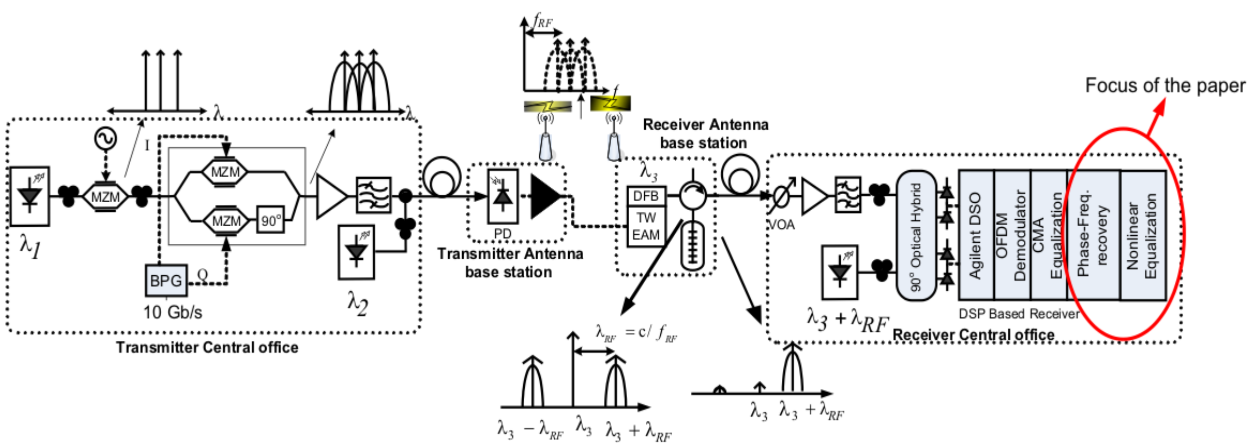

Fig.1: Experimental setup for the generation and demodulation of single and multi-carrier wireless signals. (The antennas are only for illustrative purpose and no wireless transmission was performed.) BPG: bit pattern generator, VOA: variable optical attenuator. TW-EAM: travelling wave electro-absorption modulator, DFB: Distributed feedback laser

First, a high capacity optical baseband signal is generated at λ_1. For multi-carrier optical OFDM signal generation a MZM modulator is used to generate orthogonal subcarriers. The output of the MZM is then fed into an optical I/Q modulator (nested Mach-Zehnder structure) which is driven by two independent data streams I and Q at 10 Gbaud. The modulation format for the experiment is QPSK. For the single carrier optical baseband signal, we have a capacity of 20 Gb/s and for the multi-carrier system (optical OFDM), we have two subcarriers each modulated at 20 Gb/s, resulting in a total bit rate of 40 Gb/s. The optical baseband signal is then optically amplified and sent to a photodiode where up-conversion to a RF carrier in the 75 GHz – 110 GHz band is obtained by heterodyne beating with an unmodulated CW laser at λ_2 [4]. At the antenna site, the received electrical signal in the 75 GHz – 110 GHz band is first amplified and then used to drive a travelling wave electro-absorption modulator (TW-EAM) which is integrated with a DFB laser developed in the European project HECTO. The output of the TW-EAM at λ_3 is single sideband filtered and only one sideband containing data modulation $\lambda_3 + \lambda_{RF}$, see Fig. 1, is sent to digital coherent receiver for signal demodulation, so called RF transparent demodulation [5]. In the optical hybrid, the data signal at $\lambda_3 + \lambda_{RF}$ is mixed with the LO laser ($\sim \lambda_3 + \lambda_{RF}$) and the photodeteced inphase and quadrature outputs of the photodiode are sampled at 20 Gs/s and demodulated offline.

3. Novel demodulation structure

In Fig. 2, the proposed digital carrier phase and frequency recovery structure is shown together with a nonlinear decision feedback equalizer. The novelty behind the proposed carrier phase and frequency recovery structure is that the V&V algorithm is embedded inside a digital phase-locked loop to produce an error signal for the feedback loop. The advantages of the proposed structure is that it uses blind (robust) phase estimation by employing V&V and feedback loop to track the fast phase and frequency fluctuations.

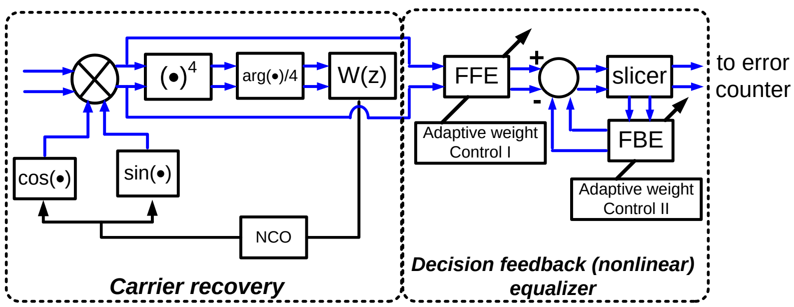

Fig. 2. Carrier phase and frequency recovery structure and nonlinear decision feedback equalizer.

The operation of the digital carrier phase and frequency recovery structure is as following. The sine/cosine processor accepts the real NCO phase samples and delivers sine and cosine samples of those phases to produce a complex locally generated signal. The phase rotator performs a complex multiplication between the incoming signal and the locally generated signal to produce complex frequency difference signal. A phase detector algorithm consist of a V&V algorithm including a digital filter W(z) and produces an error signal. The error signal is then applied to the NCO. When the structure reaches stable steady state operation, the frequency and phase difference between the transmitter and LO laser is removed from the incoming signal. The signal is then sent to a nonlinear decision feedback equalizer consisting of a feedforward filter (FFE) and feedback filter (FBE). The taps of the FFE and FBE equalizers are adjusted by LMS stochastic algorithm.

4. Experimental results

In order to test the carrier phase and frequency recovery structure shown in Fig 2, to begin with the modulation format is single carrier 20 Gb/s QPSK at 82 GHz RF carrier frequency. The receiver is tested for relatively low received optical power of -47 dBm. In Fig. 3(a), a constellation diagram of the demodulated QPSK signal is shown demonstrating that the signal can be recovered. Fig. 3(a) indicates that the four “clusters” have extended shapes illustrating that the signal is impaired by phase noise. Next, the bit error rate is plotted a function of a normalized loop gain for various values of digital filter W(z) coefficients τ_1/τ_2, see Fig. 3(b). In general, it can be observed from Fig.3(b), that by varying the normalized loop gain the BER below UFEC threshold can be obtained. Additionally, Fig.3(b) shows that there exists an optimum value for the normalized loop gain which results in the minimized BER as it is expected from the theory. By decreasing the ratio between the digital filter coefficients τ_1/τ_2, the BER becomes more invariant to the normalized loop gain. Next, using Fig. 3(b), the carrier phase and frequency recovery structure is optimized and we investigate the impact of constant modulus algorithm (CMA) on the system performance. In Fig. 4(a), the BER is plotted as a function of the length of the CMA filter for the single carrier 20 QPSK at 82 GHz and multi-carrier (2 subcarriers) OFDM signal with the bit rate of 20 Gb/s per subcarrier.

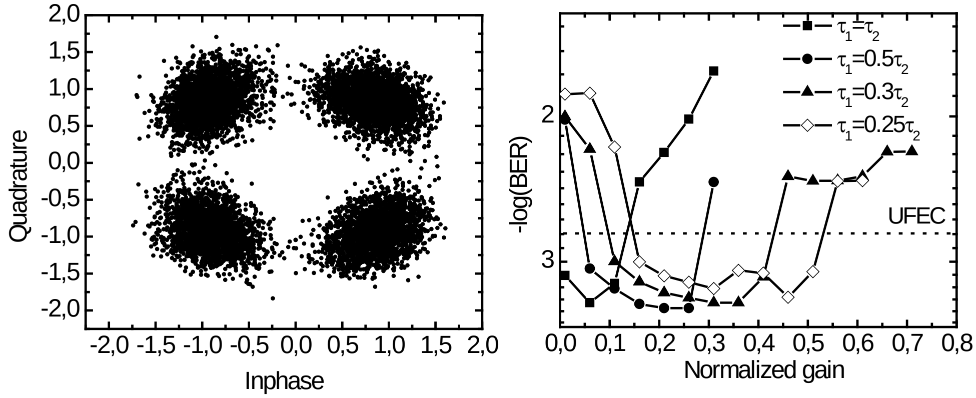

Fig. 3. (a) Constellation diagram of the recovered 20 Gb/s QPSK signal at 82 GHz RF carrier. (b) BER as a function of the normalized loop gain for various values of digital filter.

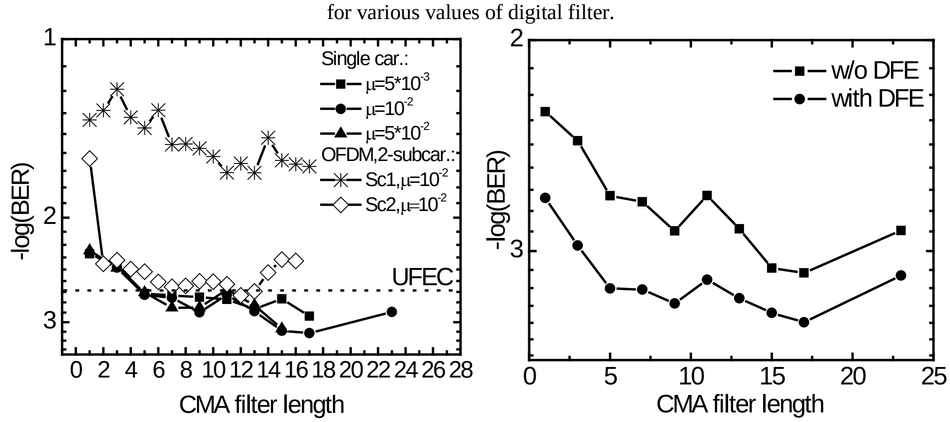

Fig. 4. (a) BER as a function of a FIR CMA digital for single carrier and multi-carrier modulation format. (b) BER as a function FIR CMA fiter with and without DFE equalizer

In general, the BER performance improves as the CMA length is increased. However, for very long filter length the CMA cannot converge due to its noise amplification. For single carrier 20 Gb/s QPSK system, we also varied the step size parameter μ and as observed that within the varied range the system is not so sensitive. For the multi carrier system with the total capacity of 40 Gb/s only one subcarrier can be obtained below UFEC threshold due to sever components limitations. However, it should be noted that the required CAM filter length is relatively small indicating the feasibility for real-time implementation. In Fig. 4(b), the BER is plotted as function of CMA filter length with and without decision feedback equalizer consisting of 1 tap for FFE and 6 taps for FBE. It can be observed from Fig 4(b), that the DFE can push down the BER and improve the overall system performance. Also, it should be noticed that the length of FBE is 6 taps compared to 1 tap for FFE indicating that the signal is impaired by nonlinearities.

5. Conclusion

We have presented a robust digital carrier phase and frequency algorithm for wireless links with capacity of up to 40 Gb/s in 75 GHz –100 GHz band. It has been experimentally demonstrated that the algorithm works pretty well in the environment severally impaired by large frequency offsets and phase noise. It has also been shown that the short nonlinear equalizer with 1 FFE tap and 6 FBE can be used to improve the system BER further.

6. References

[1] J. Wells, IEEE Microwave Magazine, **10,** (3), 104-112 (2009).
[2] Weiss M et al., International Topical Meeting on Microwave Photonics, paper CPDA8, (2009)
[3] W.-J. Jiang et al., European Conference on Optical Communication, paper Th.9.B.5, (2010)
[4] Sambaraju et. al., International Topical Meeting o Microwave Photonics, PD paper (2010).
[5] D. Zibar et al., IEEE Photonics Technology Letters **22,** (11), 784-786 (2010)